J. Phys.: Condens. Matter **8** (1996) 7073–7084. Printed in the UK

A single-crystal neutron scattering study of lattice melting in ferroelastic Na_2CO_3

M J Harris†, M T Dove‡ and K W Godfrey§

† ISIS Facility, Rutherford Appleton Laboratory, Chilton, Didcot, Oxfordshire OX11 0QX, UK
‡ Mineral Physics Group, Department of Earth Sciences, University of Cambridge, Downing Street, Cambridge CB2 3EQ, UK
§ Oxford Physics, Clarendon Laboratory, Parks Road, Oxford OX1 3PU, UK

Received 1 June 1996

Abstract. We present the results of an extensive single-crystal neutron scattering study of the ferroelastic phase transition in Na_2CO_3. This material has previously been demonstrated to undergo a continuous loss of long-range order at its ferroelastic transition, which is the phenomenon known as lattice melting. We show that our data are consistent with a special form of lattice melting where the long-range order appears to be destroyed in a two-dimensional sense, but is preserved in the third dimension.

1. Introduction

Lattice melting is an unusual effect that occurs at continuous ferroelastic phase transitions where the elastic instability is two-dimensional. In most ferroelastic transitions, the instability is one dimensional, so that at T_c, the speed of sound vanishes for propagation along a certain crystallographic direction. The order-parameter dimensionality, m, for these transitions is then equal to 1. In the two-dimensional case ($m = 2$), the speed of sound vanishes for propagation in sets of crystallographic *planes*. Hence, these sorts of ferroelastic phase transitions are driven by transverse acoustic phonons that soften over planes of wavevectors. Renormalization-group theoretical studies [1, 2] indicate that the mean-squared atomic displacements are expected to diverge at such a transition, much as they do in a conventional liquid–solid transition. However, unlike the liquid–solid transition, in the $m = 2$ transition they diverge continuously, and only along one crystallographic direction, which is the direction of the soft phonon eigenvectors. The end result is still that the crystalline long-range order is destroyed completely at T_c, but unlike a conventional melting transition it recovers after the transition is passed. This is the process known as lattice melting [3].

Mayer and Cowley [4] calculated the scattering cross section at the $m = 2$ transition, and showed that the loss of long-range order at T_c destroys the usual delta-function Bragg scattering and replaces it with diffuse scattering centred on the Bragg positions. This scattering has a finite intrinsic width and is described by a power-law singularity similar in form to that seen in two-dimensional systems such as smectic liquid crystals [5], where the long-range order is also suppressed completely by acoustic-mode fluctuations.

Despite a great deal of effort, until very recently this phenomenon had never been observed unambiguously, since there appeared to be no material that has a continuous

0953-8984/96/387073+12$19.50 © 1996 IOP Publishing Ltd

$m = 2$ phase transition. However, recent neutron powder diffraction work has shown that the ferroelastic transition at ~ 760 K in Na_2CO_3 has the correct credentials and the dramatic effect of ideal lattice melting was observed for the first time [6]. The symmetry change at this phase transition is $P6_3/mmc - C2/m$, and the order parameter is the ϵ_5 shear strain. Detailed structure refinements [7] show that the order parameter goes to zero smoothly at T_c. This is consistent with the transition being second order, and therefore continuous.

The crystal structure of the hexagonal phase of Na_2CO_3 contains one-dimensional chains of NaO_6 face-sharing octahedra lying parallel to the $\boldsymbol{c}$-axis. These chains are linked to each other laterally by carbonate groups that lie parallel to the (0 0 1) planes [3, 7]. One can imagine that the restoring force for shear motions of the chains against each other (with the carbonate groups acting as 'hinges') is relatively small, and indeed, this is how the ferroelastic transition is accomplished: as the crystal is cooled towards T_c the restoring force becomes smaller and smaller, and the shear fluctuations larger in amplitude, until eventually the critical point is reached. Below this temperature, the shear fluctuations freeze in, to produce the static monoclinic strain. These shear fluctuations are the critical acoustic modes, which are transverse acoustic modes with wavevectors in the $\boldsymbol{a}^*$–$\boldsymbol{b}^*$ plane, and with eigenvectors parallel to the $\boldsymbol{c}$-axis. Hence, the process of lattice melting is largely a divergence of the mean-squared atomic displacements along the $\boldsymbol{c}$-axis.

A preliminary single-crystal neutron diffraction study of the ferroelastic phase transition has been published recently, providing further confirmation of this unusual effect [8]. In this paper, we provide a detailed analysis and discussion of the single-crystal neutron scattering data and show that they are fully consistent with the theoretical predictions.

2. Experimental details

The crystals for this work were grown by the Czochralski technique. This took place inside a stainless steel chamber filled with nitrogen gas to a pressure of 1.1 bar, using a 6 kW radio frequency generator induction heater. A 50 cc platinum crucible was charged with approximately 55 g of sodium carbonate powder (Johnson Matthey 'ultrapure') over a period of four pre-meltings in the Czochralski chamber, out-gassing each time to 7×10^{-7} torr. The material was melted (where the melting point is at 1124 K) at approximately 30% of the generator's full power.

With small adjustments in the generator power, initial nucleation was obtained on a cooled platinum wire dipped into the melt. With the power being constantly monitored and adjusted to maintain a good boule shape, a transparent and colourless crystal approximately 20 mm in length and about 15 mm diameter was pulled at 20 mm h^{-1}, while being rotated at 60 rpm. When the required size of boule was obtained it was removed from the surface of the melt and the crucible was then cooled to room temperature at approximately 100 K h^{-1}. On cooling through the ferroelastic and incommensurate phase transitions [9], the crystal became opaque and milky in appearance. A typical crystal has a mass of approximately 6 g.

Neutron scattering experiments were performed using the PRISMA time-of-flight spectrometer at the ISIS neutron facility (Rutherford Appleton Laboratory). Temperature control was provided by a water-cooled furnace with vanadium windows. The crystal was held in place inside the furnace by a tantalum strap attached to the furnace centre-stick. As much of the strap and centre-stick as possible was shielded from the neutron beam with gadolinium foil. Rocking curves were performed at room temperature to check the crystal quality, and the mosaic spread of the crystal was found to be about 0.4°.

In its diffraction mode, PRISMA allows for a number of simultaneous radial scans in

reciprocal space to be performed with just a single setting of the crystal and instrument. By measuring several crystal settings in turn, one may build up rapidly a data set which consists of a two-dimensional mesh of points. Each radial scan in a setting includes an integration over all inelastic processes up to a certain energy, which is a function of the particular wavevector-transfer along each scan. The crystal of Na_2CO_3 was oriented so that the scattering plane was the $\boldsymbol{a}^*$–$\boldsymbol{c}^*$ plane, and radial scans were performed over the (0 0 2), (0 0 4), (0 0 6) and (0 0 8) reflections. The energy integration at these positions is performed over a range of about 2.5, 10, 22 and 41 THz, respectively. This is more than adequate to integrate over all of the critical acoustic modes close to T_c, and so we are confident that the line profiles of each peak contain all of the scattering from the critical modes.

We have also performed a preliminary study of the temperature dependence of the transverse and longitudinal acoustic phonon branches around the (0 0 2) peak, using PRISMA operating in its inelastic mode. Twelve detector–analyser arms were used, each with an analysing energy of 4.35 THz, which resulted in a resolution width of about 0.24 THz (FWHM) at zero energy transfer. Since PRISMA uses the time-of-flight principle, each detector–analyser arm measures an oblique trajectory through ($\boldsymbol{Q}$, E)-space. We were interested in obtaining the dispersions of the transverse acoustic mode in the $\boldsymbol{a}^*$–$\boldsymbol{b}^*$ plane and the longitudinal acoustic mode in the $\boldsymbol{c}^*$ direction as a function of temperature. Rather than performing a series of constant-Q scans along the symmetry directions, we configured the spectrometer so that we could make use of all 12 inelastic detectors simultaneously, by performing scans that intersected with the acoustic dispersion surface at a series of arbitrary points around the (0 0 2) position. The observed phonon peaks then gave us a set of ($\boldsymbol{Q}$, E) points which we fitted with a simple harmonic model for the whole dispersion surface. This enabled us to determine the temperature dependences of the C_{33} and C_{44} elastic constants, which are presented in section 4.

In this experiment, we found that T_c was at a measured sample temperature of 760.6 K, rather than 755 K, as in the powder experiment. This is due to the fact that it is rather difficult to measure the temperature accurately in a neutron scattering experiment, because of the relative size of the sample and the necessity to keep the thermocouple as far out of the neutron beam as is practical. Hence, while measurements of the relative temperature in a particular experiment are generally reliable, discrepancies often arise when comparisons of the results from two different experiments are made.

3. Neutron diffraction results

The effect of lattice melting in Na_2CO_3 is to replace the sharp Bragg peaks by broad scattering profiles with a cusp-shaped distribution (a power-law singularity in the wavevector, to be precise) perpendicular to the $\boldsymbol{c}^*$ direction, as we discuss in section 3.1.

In figure 1, we show the scattering at the (0 0 4) position as contour plots for three different sample temperatures. The profile of the scattering measured at temperatures far from the transition temperature is dominated by the experimental resolution function. This is illustrated in the first plot, for a sample temperature of 893 K. Note that the tail extending to lower wavevectors along [0 0 ℓ] is due to the asymmetric distribution of neutron energies in the incident neutron pulse, and so is contained in the experimental resolution function. As the sample is cooled towards T_c, strong diffuse scattering appears extending outwards from the main diffraction peak in the $\boldsymbol{a}^*$–$\boldsymbol{b}^*$ plane of wavevectors (i.e. for [h 0 4] wavevectors in the plot). This is due to the softening transverse acoustic mode and at the transition

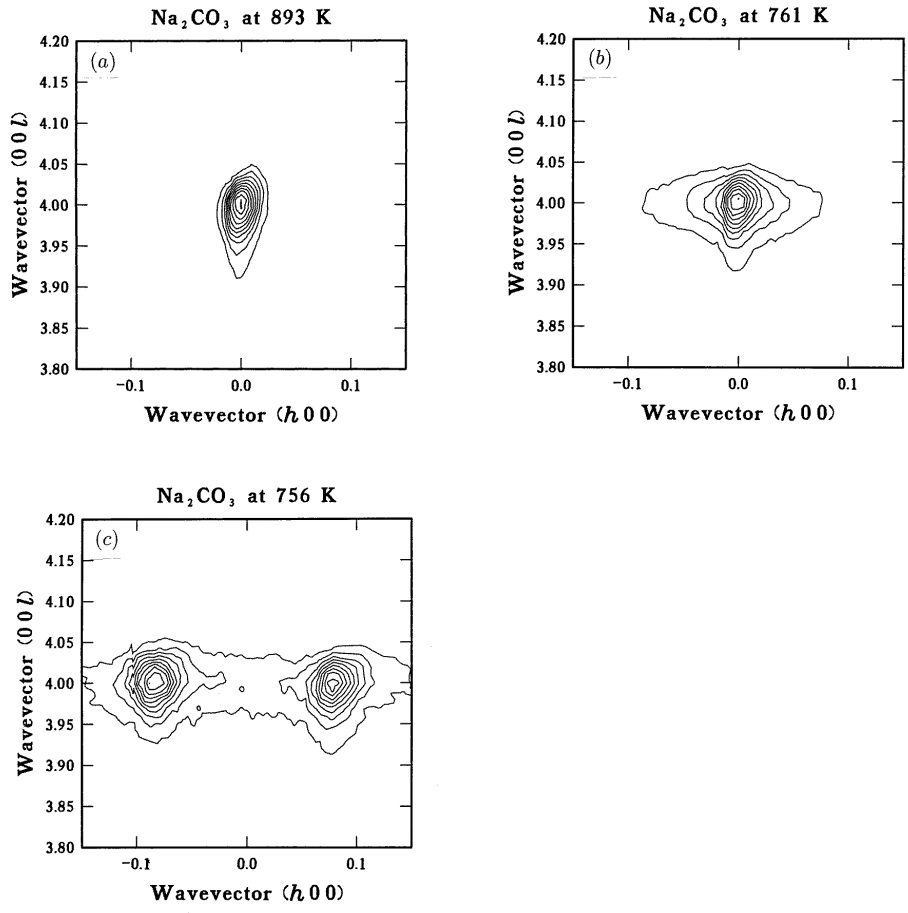

Figure 1. Contour plots of the neutron scattering from Na_2CO_3 around the (0 0 4) position at (*a*) temperatures well above (893 K), (*b*) just above (761 K) and (*c*) below (756 K) the ferroelastic transition. The lattice melting is evident as significant diffuse scattering perpendicular to the $\boldsymbol{c}^*$-axis.

temperature the scattering takes on a cusp-shaped distribution. This is apparent from the data taken at a sample temperature of 761 K, which is 0.4 K above T_c. In the third plot in figure 1, we show the scattering observed at 4.6 K below the transition temperature. This is now in the monoclinic phase, and the (0 0 4) peak has split due to ferroelastic twinning of the crystal. There is still significant diffuse scattering in the $\boldsymbol{a}^*$–$\boldsymbol{b}^*$ plane, but the cusp-shaped profiles of the diffraction peaks have disappeared, and the scattering is again dominated by sharp, resolution-limited Bragg scattering. Note that no diffuse scattering is observed to appear along the [0 0 ℓ] direction at any temperature.

3.1. The scattering cross section

The scattering cross section for a crystal at the critical temperature of an $m = 2$ ferroelastic transition was investigated by Mayer and Cowley [4] and obtained analytically. The starting

point is the energy-integrated scattering function for a crystal with atoms i, j:

$$S(\boldsymbol{Q}) = \sum_{i,j} b_i b_j \exp(\mathrm{i}\boldsymbol{Q} \cdot [\boldsymbol{r}_i - \boldsymbol{r}_j]) \exp(-F) \tag{1}$$

with

$$F = \tfrac{1}{2}\left\langle (\boldsymbol{Q} \cdot [\boldsymbol{u}_i - \boldsymbol{u}_j])^2 \right\rangle \tag{2}$$

where b_i is the form factor for atom i, $\boldsymbol{r}_i$ gives its equilibrium position, $\boldsymbol{u}_i$ is the displacement due to the phonon modes, $\boldsymbol{Q}$ is the wavevector transfer and the brackets $\langle \cdots \rangle$ indicate the thermal average. The usual procedure for calculating the scattering cross section is to expand the exponent, F, for the second exponential as a power series in the small displacements $\boldsymbol{u}_i$. However, for the continuous $m = 2$ transition this approach fails because the displacements corresponding to the soft modes diverge in amplitude at T_c. These soft modes are transverse acoustic modes that have eigenvectors parallel to the [0 0 1] direction and wavevectors in the $\boldsymbol{a}^*$–$\boldsymbol{b}^*$ plane (which hereafter we shall refer to as the 'critical plane'). Mayer and Cowley [4] overcame the problem of how to calculate the scattering law when some displacements are divergent by separating F into a critical and a non-critical part. The non-critical part may be obtained with the usual expansion, but the critical part requires an integration over the critical acoustic modes with propagation directions in and close to the critical plane, up to a cut-off wavevector, Λ. The phonon frequency, ω, of the critical branch may be written within mean-field theory as

$$\omega^2 = q_\perp^2 \left(v^2 + \lambda q_\perp^2\right) + w q_\parallel^2 \tag{3}$$

where $\boldsymbol{q}_\parallel$ and $\boldsymbol{q}_\perp$ are the wavevectors parallel and perpendicular to the $\boldsymbol{c}^*$ axis, v is the soft velocity of sound, and λ and w are related to the non-soft elastic constants. Note that we define $\boldsymbol{q}_\parallel$ and $\boldsymbol{q}_\perp$ in the opposite sense from Mayer and Cowley. At the critical temperature, it is possible to obtain an analytical solution for the scattering law, and close to a reciprocal lattice vector $\boldsymbol{G}$, this is

$$S(\boldsymbol{G} + \boldsymbol{q}_\perp) \sim q_\perp^{-2\alpha} \tag{4}$$

and

$$S(\boldsymbol{G} + \boldsymbol{q}_\parallel) \sim q_\parallel^{-\alpha}\,. \tag{5}$$

The exponent α is given as

$$\alpha = 2 - a(\boldsymbol{G}) \tag{6}$$

where

$$a(\boldsymbol{G}) = \frac{k_B T G_\parallel^2}{4\pi\rho\,(w\lambda)^{1/2}}\,. \tag{7}$$

k_B is Boltzmann's constant, T is the temperature, $G_\parallel$ is the component of the wavevector transfer along $\boldsymbol{c}^*$ and ρ is the density.

Dove *et al* [10] have performed lattice dynamics calculations to investigate whether the driving force behind the ferroelastic transition in Na_2CO_3 is an optic or an acoustic mode instability. In the case of an optic mode instability, the transverse acoustic mode is coupled to a softening optic mode which drives the transition. In the acoustic mode case, the transverse acoustic mode is soft of its own accord. Dove *et al* [10] showed that in the case of Na_2CO_3, a straightforward acoustic instability occurs, but over a plane so that the C_{44} elastic constant softens to zero over *all* wavevectors in the $\boldsymbol{a}^*$–$\boldsymbol{b}^*$ plane. The end result is that the dispersion parameter λ is very close to zero. In the following discussion, we assume that λ is indeed zero for Na_2CO_3 and we have analysed our diffraction data

accordingly. We present further justification for this approach later. In the instance that $\lambda \sim 0$, Mayer and Cowley show that the scattering function is modified to

$$S(\boldsymbol{G}+\boldsymbol{q}) \sim \delta(q_{\parallel}) q_{\perp}^{-\alpha} \tag{8}$$

where the $\delta\left(q_{\parallel}\right)$ is the Dirac delta function in the non-critical wavevector $\boldsymbol{q}_{\parallel}$. Hence, the scattering is sharp perpendicular to the plane of soft wavevectors, but has the power-law form within it, as we have observed experimentally for Na_2CO_3 within the limits of the experimental resolution.

These results show that the scattering from a *three-dimensional* crystal undergoing a continuous $m = 2$ ferroelastic transition takes the form of a power-law singularity, rather than the delta function characteristic of Bragg scattering resulting from long-range crystallographic order. This scattering law is identical with the corresponding expression for the scattering from *two-dimensional systems* such as a smectic liquid crystal [5] and a two-dimensional crystal below the Kosterlitz–Thouless transition [11].

However, at temperatures above and below T_c, there is no analytical solution for the scattering function and it must be calculated numerically, which was the approach that we have adopted in analysing our neutron diffraction data. Continuing with the treatment of Mayer and Cowley [4], the argument of the second exponential in (1) is

$$F = a(\boldsymbol{G}) \int_0^{\Lambda} \mathrm{d}k \frac{1 - J_0(k u_{\perp})}{\left(\kappa^2 + k^2\right)^{1/2}} \tag{9}$$

where $J_0(k u_{\perp})$ is the zeroth-order Bessel function with an argument which is the product of a wavevector and a displacement perpendicular to the eigenvector of the critical mode. κ is the so-called inverse correlation length, which is defined as

$$\kappa = v\lambda^{-1/2}. \tag{10}$$

κ is thus proportional to $C_{44}^{1/2}$, the square root of the soft elastic constant, and it controls the temperature dependence of the scattering function.

3.2. Analysis of the neutron diffraction data

In the data analysis procedure, we concentrated on the scattering at (0 0 4). This is because of the wavevector dependence of the exponent α in the scattering law: for the (0 0 2) position we found that the exponent is very close to that expected for diffuse scattering from non-critical acoustic modes (which follows the approximate law $S(q) \sim q^{-2}$), while for the (0 0 6) position the exponent is so close to zero that the diffuse scattering at T_c is spread out over a large portion of reciprocal space and its intensity is rather weak. The scattering at (0 0 4) on the other hand is reasonably strong and has a value of α significantly less than 2, so that it is favourable for investigating the effects of lattice melting.

In figure 2 we show cuts through the data sets along $\boldsymbol{q}_{\perp}$ through the (0 0 4) peak for three different temperatures. For the highest temperature shown (893 K) the scattering consists predominantly of sharp Bragg scattering, with weak wings of diffuse scattering due to the softening transverse acoustic modes. As the sample is cooled towards T_c, the Bragg scattering weakens while the diffuse scattering from the acoustic modes along $\boldsymbol{q}_{\perp}$ becomes stronger. At 761 K the Bragg scattering is entirely replaced by diffuse scattering with a cusp-shaped distribution, reflecting the power-law singularity in (8). Below T_c, the scattering sharpens up again as the diffuse scattering dies away, to be replaced by Bragg scattering. This process reveals the onset of continuous lattice melting at the phase transition, with the recovery of long-range order once the transition is passed. In figure 3 we show the

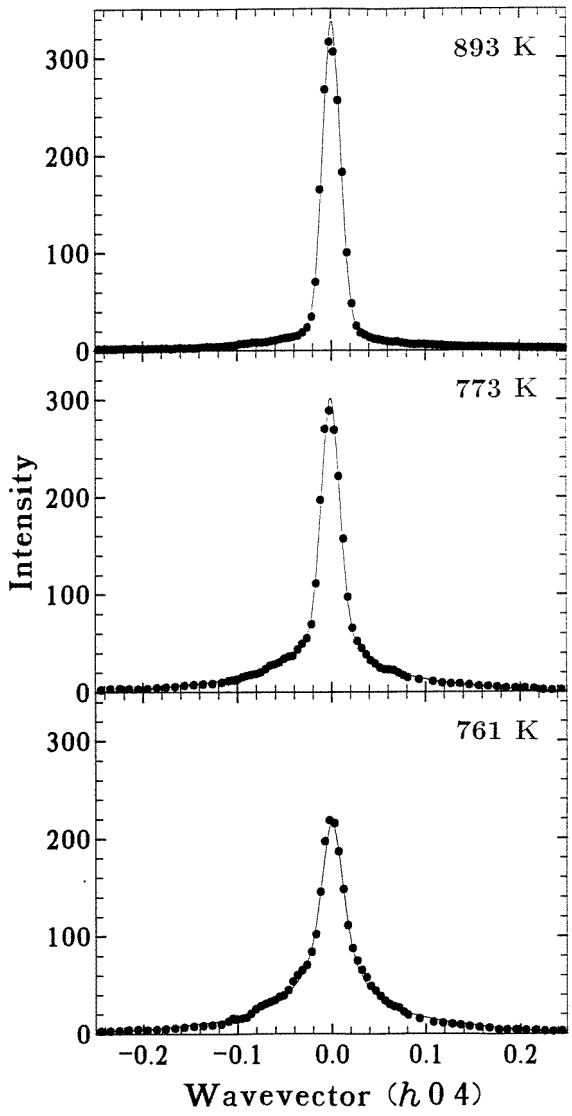

Figure 2. Transverse (h 0 4) cuts for sample temperatures 893, 773 and 761 K, with T_c = 760.6(3) K. The curves are the results of fits to the data of the Mayer–Cowley scattering function, convoluted with the experimental resolution function. The 761 K data have a clear cusp-shaped distribution, due to the power-law singularity in the scattering law. The 893 K data show strong Bragg scattering with weak wings of diffuse scattering from the transverse acoustic modes. The data taken with a sample temperature of 773 K show an intermediate situation.

scattering along the $q_\parallel$ direction through the (0 0 4) position. Note that the asymmetric peak shape for the scattering along this direction arises from the fact that PRISMA utilizes a white incident neutron beam which has a strongly asymmetric distribution of neutron energies. No significant diffuse scattering or broadening beyond the limit of the experimental resolution function is observed at any temperature, supporting our assumption that $\lambda \simeq 0$ for Na_2CO_3,

so that the scattering at the transition point is described by (8).

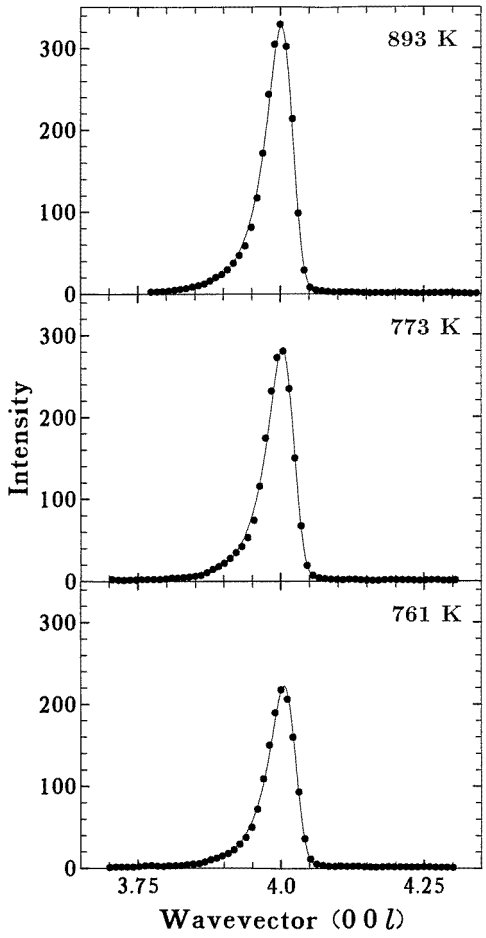

Figure 3. Longitudinal (0 0 ℓ) cuts through the (0 0 4) position for the sample temperatures 893, 773 and 761 K. The curves are the results of fits to the data simply of the experimental resolution function. Within the experimental resolution, the scattering law appears to be delta-function-like at these three temperatures.

The curves in figure 2 are fits to the data of the Mayer–Cowley scattering function, expression (1), convoluted with the experimental resolution function. The free parameters in each fit were a flat background, a centre (to allow for slight misalignment errors), a scale factor, and κ, the Mayer–Cowley correlation length. In this calculation the integral over the critical modes, i.e. F in equation (9), is performed from 0 to a cut-off wavevector Λ. It was found that as Λ was increased, the wings of diffuse scattering at large values of $\boldsymbol{q}_\perp$ become stronger. This is because Λ effectively controls the contribution of the acoustic modes to the scattering in the wings. We varied Λ until the calculation predicted negligible diffuse scattering for values of $\boldsymbol{q}_\perp$ beyond 0.3, consistent with our experimental observations, and then it was held fixed in all fits to the data. We found that the value of Λ that gives the best agreement with the experimental data is 0.27 Å^{-1}. This value shows

that the main contribution to the scattering comes from the transverse acoustic modes in the region between the zone centre and out to about half the distance to the zone boundary.

Also required was the value of the parameter $a(\boldsymbol{G})$, which controls the exponent of the power law along $\boldsymbol{q}_\perp$ (expressions (6) and (7)). This was determined from the data set obtained closest to the transition temperature (which was the 761 K data set), because of the dominance of the power-law diffuse scattering close to the transition. a was then kept fixed in all subsequent fits. We found that the value of a for the (0 0 4) peak is 0.78(2) at T_c. Using equation (7), this predicts that the values of a for the (0 0 2) and (0 0 6) peaks are 0.20 and 1.76, respectively. These values were found to be in excellent agreement with the observed scattering at these positions. For the (0 0 8) position, equation (7) predicts that $a > 2$, which means that there is no longer a power-law singularity at this point, and the scattering is finite for all $\boldsymbol{q}_\perp$, like a liquid structure factor. The experimental observations are in agreement with this, since there is no trace of any significant scattering at the (0 0 8) position above the level of the background.

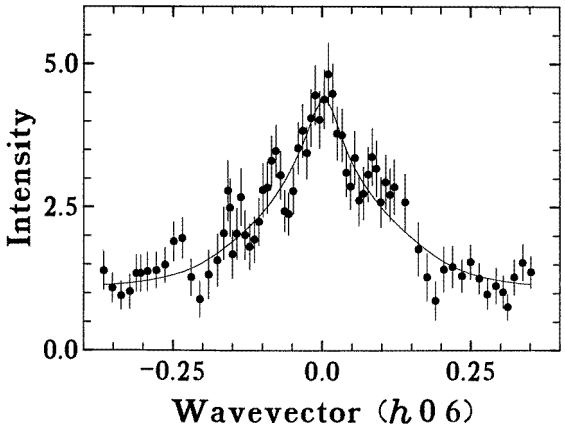

Figure 4. A transverse cut through the scattering at the (0 0 6) position at a sample temperature of 762 K. The curve is a fit to the data of the Mayer–Cowley scattering function, with parameters obtained from the analysis of the (0 0 4) scattering.

The fits to the observed data of the Mayer–Cowley model are excellent. As stated above, we concentrated on the scattering at the (0 0 4) position, but found that the model also gives a very good description of the scattering at the (0 0 2) and (0 0 6) positions. For instance, in figure 4 we show the scattering at the (0 0 6) position at a temperature of 762 K, together with a fit of the Mayer–Cowley function. The parameters used were obtained from the analysis of the (0 0 4) data, so that $\kappa = 0.10$ and $a = 1.76$. These were then kept fixed in the fit, and the only parameters that were allowed to vary were a flat background, a centre and a scale factor. The agreement factor obtained was $\chi^2 = 0.95$. The fact that we obtain such good agreements for the (0 0 2) and (0 0 6) scattering, as well as for that at (0 0 4) indicates that our assumption that $\lambda \sim 0$ is correct, and that the scattering at the transition may be approximated well by equation (8). The alternative more general scattering law (equation (4)) is wholly inappropriate. If we had used this law, we would have found that the exponent $\alpha = 0.61$ for the (0 0 4) peak, so that $a = 1.39$. Applying equation (7), we would then find that for the (0 0 6) position, $a = 3.13$. However, this value of a cannot be physically correct, because it means that the exponent $\alpha = -1.13$, and there would then be

no divergence in the scattering at the (0 0 6) position. There must be a divergence, since we observe a peak in the scattering at this position for all temperatures. This strengthens our claims that the scattering law with $\lambda \sim 0$ (i.e. equation (8)) is appropriate.

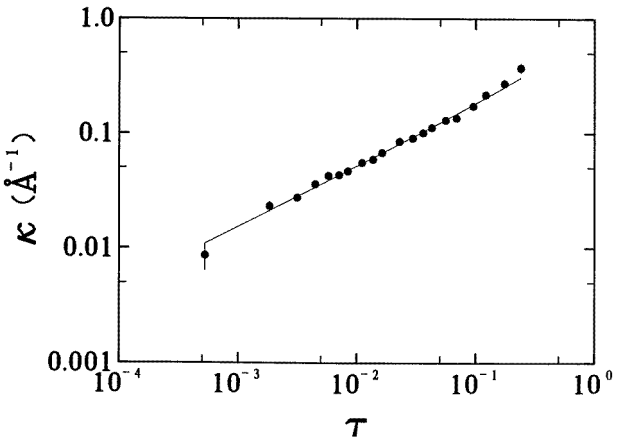

Figure 5. Temperature dependence of the inverse correlation length, κ. Note that the reduced temperature $\tau = (T - T_c)/T_c$. The curve is a fit of the expected temperature dependence of κ (equation (11)).

In figure 5, we show the values of κ obtained from the fits. Since κ is essentially the inverse correlation length for the low-temperature phase, it should have the following temperature dependence:

$$\kappa \propto \tau^{1/2} |\ln \tau|^{-1/6} \tag{11}$$

with the reduced temperature $\tau = (T - T_c)/T_c$. The logarithmic correction arises from the fact that the transition belongs to the $m = 2$ universality class [1, 2]. The curve in figure 5 shows a fit of this temperature dependence to the values of κ. The agreement factor for the fit was $\chi^2 = 1.1$ and the transition temperature, T_c, was obtained as 760.6(3) K. We note that an attempt to fit the data without the logarithmic correction in the above expression for κ gives a somewhat poorer agreement factor, thus providing further support for the argument that logarithmic corrections to the critical properties must be made for $m = 2$ transitions.

4. Inelastic neutron scattering results

The above analysis of the single-crystal neutron diffraction data hinges on whether our assumption that $\lambda \simeq 0$ is valid or not. We have already discussed various justifications for this assumption. We will now present preliminary measurements of the temperature dependences of the C_{33} and C_{44} elastic constants, which add further weight to our argument.

In figure 6, we show the temperature dependences of the C_{33} and C_{44} elastic constants. C_{33} softens gently as the temperature is increased, reflecting the non-critical thermal expansion of the crystal. However, C_{44} is clearly the critical elastic constant, because it softens towards zero on cooling towards T_c. Unfortunately, apart from the highest-temperature data point, the fitted values for C_{44} are slightly underestimated because of the difficulty in fitting to a very small frequency in the presence of much larger frequencies; the

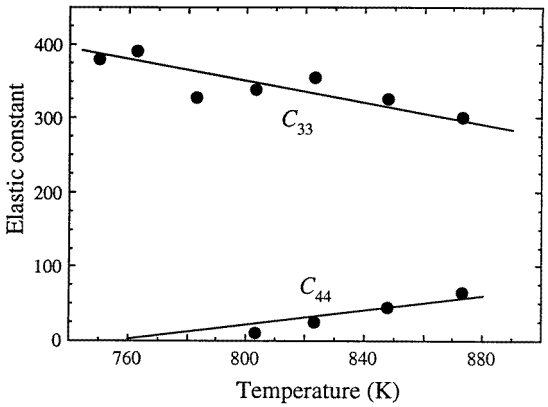

Figure 6. Temperature dependences of the C_{33} and C_{44} elastic constants in Na_2CO_3, as obtained by inelastic neutron scattering measurements. The elastic constants are displayed in units of $THz^2\,Å^2$. The lines are guides to the eye. The line for C_{44} is chosen to pass through the highest-temperature data point and T_c.

highest-temperature value of C_{44} is reliable, because we have inelastic data that is almost from the pure transverse acoustic mode.

Using the behaviour of the C_{33} elastic constant, we have obtained a value for the dispersion parameter w (equation (3)) at the transition. We can then calculate λ, using the parameter a that we have determined from the diffraction measurements (equation (7)). If we assume that λ is small, so that equation (8) holds for describing the diffraction profile at the transition, then we find that $\lambda = 26.8\ THz^2\,Å^4$. However, if we say that the diffraction profile in the plane of critical wavevectors is given by the more general scattering law (equation (4)), we find that $\lambda = 8.5\ THz^2\,Å^4$. These two values are of the same order. The question is, how small does λ have to be before we can assume that $\lambda \sim 0$, so that equation (8) holds? Mayer and Cowley [4] use λ to define a non-critical length, $d = (\lambda/w)^{1/2}$, which is essentially the length scale of the correlations in the plane perpendicular to the direction of the diverging mean-squared atomic displacements. This length scale is then about 1.3 Å. However, d contains a factor of 2π in the denominator, so converting it to a real distance gives us the length scale 8 Å. Hence, the correlations perpendicular to the diverging displacements are of the order of only a single unit cell. This is to be expected, since the fluctuations that occur at the transition point are large-scale uncorrelated shears of the chains of octahedra against each other along the $\boldsymbol{c}$-axis. Our non-critical length scale is then effectively the diameter of a single chain, which is approximately what we find. We therefore feel confident that our treatment of the Na_2CO_3 diffraction data, where we assumed that $\lambda \sim 0$, is valid.

5. Conclusions

We have presented results from combined single-crystal neutron diffraction and inelastic neutron scattering experiments on the ferroelastic phase transition in Na_2CO_3. These results have allowed us to test rigorously the theoretical predictions of Mayer and Cowley [4]. We find an excellent agreement between our observations and these predictions, indicating that complete lattice melting occurs in Na_2CO_3. This involves a continuous divergence of the mean-squared atomic displacements at the ferroelastic transition, so that the crystalline long-

range order is destroyed and Bragg scattering is replaced by diffuse scattering with a finite intrinsic width. We find that Na_2CO_3 approximates to a special case of the Mayer–Cowley theory where, rather than softening only around the zone centre, the critical transverse acoustic branch softens for all wavevectors in the critical plane. This means that the long-range order is only destroyed in a two-dimensional sense and is preserved parallel to the crystallographic $\boldsymbol{c}$-axis.

Acknowledgments

The authors thank Professor R A Cowley and Drs M E Hagen and U Steigenberger for invaluable discussions. The financial support of the EPSRC is gratefully acknowledged.

References

[1] Cowley R A 1976 *Phys. Rev.* B **13** 4877
[2] Folk R, Iro H and Schwabl F 1976 *Z. Phys.* B **25** 69; *Phys. Lett.* **57A** 112
[3] Harris M J and Dove M T 1995 *Mod. Phys. Lett.* B **9** 67
[4] Mayer A P and Cowley R A 1988 *J. Phys.: Condens. Matter* **21** 4827
[5] Als-Nielsen J, Litster J D, Birgeneau R J, Kaplan M, Safinya C R, Lindegaard-Andersen A and Mathiesen S 1980 *Phys. Rev.* B **22** 312
[6] Harris M J, Cowley R A, Swainson I P and Dove M T 1993 *Phys. Rev. Lett.* **71** 2939
[7] Swainson I P, Dove M T and Harris M J 1995 *J. Phys.: Condens. Matter* **7** 4395
[8] Harris M J, Dove M T and Godfrey K W 1995 *Phys. Rev.* B **51** 6758
[9] Harris M J and Salje E K H 1992 *J. Phys.: Condens. Matter* **4** 4399
[10] M T Dove, A P Giddy and V Heine 1992 *Ferroelectrics* **136** 33
[11] J M Kosterlitz and D J Thouless 1973 *J. Phys.: Condens. Matter* **6** 1181